

# Uniaxial crystal interferometer: principles and forecasted applications to imaging astrometry

Gabriel Y. Sirat<sup>1,2</sup>, Kalman Wilner<sup>2</sup> and Daniel Neuhauser<sup>1</sup>

<sup>1</sup>Department of Chemistry and Biochemistry,  
University of California Los Angeles CA 90095-1569 USA

<sup>2</sup>OPTIMET, 6 Hartum St, Jerusalem 91450, Israel  
[dxn@chem.ucla.edu](mailto:dxn@chem.ucla.edu)

**Abstract:** We propose a new approach to imaging astrometry, the uniaxial crystal interferometer (UCI). It uses the extremely sensitive dependence of the polarization phase change on the incident angle in uniaxial crystals. This is further combined with very sensitive polarization measurements. The polarization-coding is used for a fine-scale angle determination, and is simultaneously combined with a crude measurement through a standard telescope. Further, achromatic anamorphic prisms will amplify five to tenfold the resolution which is estimated to reach the scale ratio of large interferometers. Because the fine angular information is superimposed on the light at an early stage the optical system tolerances are relieved to the level of a standard low-weight optical imaging system. We also suggest solutions to make the system achromatic. Overall the system may cover sky segments of the order of fractions of a degree square and reach a resolution of tens of  $\mu$ as, even for faint stars.

©2005 Optical Society of America

**OCIS codes:** (350.1270) Astronomy and astrophysics, (120.2130) Ellipsometry and polarimetry, (090.2880) Holographic interferometry

---

## References and links

1. J. E. Baldwin, R.C.B., G. C. Cox, C. A. Haniff, J. Rogers, P. J. Warner, D. M. A. Wilson, and C. D. Mackay, "Design and performance of COAST," *Proc. SPIE* **2200**, 118-128 (1994).
2. Bradley, A., et al., "The Flight Hardware And Ground System For Hubble Space Telescope Astrometry," *Publications Of The Astronomical Society Of The Pacific* **103**, 317-335 (1991).
3. Benedict, G.F., et al., "Astrometry With Hubble-Space-Telescope Fine Guidance Sensor Number-3 - Position-Mode Stability And Precision," *Publications Of The Astronomical Society Of The Pacific* **106**, 327-336 (1994).
4. Unwin, S.C., et al., "Quasar astrophysics with the Space Interferometry Mission," *Publications Of The Astronomical Society Of Australia* **19**, 5-9 (2002).
5. Lindegren, L. and M.A.C. Perryman, "GAIA: Global astrometric interferometer for astrophysics," *Astronomy & Astrophysics Supplement Series* **116**, 579-595 (1996).
6. Thomas, E., et al., "Optical configuration for a micro-arcsecond astrometric interferometer in space," *Astronomy & Astrophysics supplement series* **138**, 147-154 (1999).
7. Röser, S., *Diva - Towards Microarcsecond Global Astrometry*. (1997).
8. Loiseau, S. and S. Shaklan, "Optical design, modelling and tolerancing of a Fizeau interferometer dedicated to Astronomy," *Astronomy & Astrophysics* **117**, 167-178 (1996).
9. Gai, M., M.G. Lattanzi, and G. Mana, "A Fizeau interferometer for Astrometry in space: the metrological point of view," *Measurement Science and technology* **10**, 1254-1260 (1999).
10. Sirat, G. and D. Psaltis, "Conoscopic Holography," *Opt. Lett.* **10**, 4-6 (1985).
11. Sirat, G.Y., Vecht, Jacob and Malet, Yann, "Linear conoscopic holography," US. (1999).
12. Gai, M., et al., "Location accuracy limitations for CCD cameras," *Astronomy & Astrophysics* **367**, 362-370 (2001).
13. Obeso, F., et al., "Novel on-line surface quality control for hot slabs in continuous casting," *Revue De Metallurgie-Cahiers D Informations Techniques* **99**, 267-275 (2002).
14. VanWongerghem, B., et al., "Recent performance results of the national ignition facility Beamlet demonstration project," *Fusion technology* **30**, 642-647 (1996).
15. Widmayer, C., et al., "Producing National Ignition Facility (NIF)-quality beams on the Nova and Beamlet Lasers," *Fusion technology* **30**, 464-470 (1996).

16. Zaitseva, N. and L. Carman, "Rapid growth of KDP-type crystals," Progress in crystal growth and characterization of materials **43**, 1-118 (2001).
17. Auerbach, J., et al., "Modeling of frequency doubling and tripling with measured crystal spatial refractive-index nonuniformities," Appl. Opt. **40**, 1404-1411 (2001).
18. Wegner, P.J., et al. "Frequency converter development for the National Ignition Facility," in Proc. SPIE **3492**, 392-405, Third International Conference on Solid State Lasers for Application to Inertial Confinement Fusion, W. H. Lowdermilk; Ed. 1999.
19. Sirat, G., "Conoscopic holography.1. Basic principles and physical basis," J. Opt. Soc. Am. A **9**, 70-83 (1992).
20. Li, G., et al., "Study on rapid growth of KH<sub>2</sub>PO<sub>4</sub> and its characterization," Crystal research and technology **40**, 217-221 (2005).
21. Keller, C.U., "Recent progress in imaging polarimetry," Solar Physics **164**, 243-252 (1996).
22. Keller, C.U., *Charge Caching CMOS detector for Polarimetry (C3Po)*. 2005.
23. Phillion, D.W., "General methods for generating phase-shifting interferometry algorithms," Appl. Opt. **36**, 8098-8115 (1997).
24. Trebino, R., C. Barker, and A. Siegman, "Achromatic N-Prism beam expanders - optimal configurations II," Proc. SPIE **540**, 104-109 (1985).
25. Duarte, F., "Multiple-prism arrays in laser optics," Am. J. Phys. **68**, 162-166 (2000).
26. Scholz, R.D. and U. Bastian. "Simulated dispersion fringes of an astrometric space interferometry mission," in Hipparcos Venice 97. 1997. Venice.
27. Hog, E., C. Fabricius, and V.V. Makarov, "Astrometry from space: New design of the Gaia mission," Experimental Astronomy **7**, 101-115 (1997).
28. Boulbry, B., et al., "Polarization errors associated with zero-order achromatic quarter-wave plates in the whole visible spectral range," Opt. Express **9**, 225-235 (2001).

## 1 Introduction

### 1.1 Astrometry

The survey of precise positions of a large number of stars is an active field. An important milestone was the cataloguing of more than 100000 stars positions and parallax information by Hipparcos. For further advances, several direct imaging and interferometric systems have been implemented or are planned. COAST was one of the first systems built on earth [1]. In space, the Fine Guidance Sensor of the Hubble telescope [2, 3] permits star parallax measurement with an accuracy of 1000  $\mu$ s.

The most ambitious projects are SIM – Space Interferometry mission - [4] and GAIA - Global Astrometric Interferometer for Astrophysics [5],[6]. These two projects aim at reaching a few  $\mu$ s precision. DIVA — Deutsch Interferometer für Vielkanalphotometrie and Astrometrie [7] and OSIRIS - Optical Stellar Interferometer for Russian Investigations in the Space - are simpler systems, with much lower payloads, aimed at improving the results of Hipparcos.

All proposed or developed optical systems for astrometry are based on direct imaging, as in Hipparcos or in the final version of GAIA, or use interferometry. Interferometer based systems use either a Michelson stellar (SIM and OSIRIS) or a Fizeau interferometer (DIVA). However, all these systems require a huge ancillary instrumentation. The tolerance for GAIA, for some parameters, is in the 20 pm range[8, 9]. The existing systems measure the position of a star through spatial fringes or through evaluation of the centroid of the Airy disk as in the final versions of GAIA.[9].

### 1.2 Uniaxial crystal interferometer (UCI)

UCI is an alternative to a Michelson and Fizeau interferometers which retrieves the angular position from a single wavefront. In essence, position information is coded in UCI, interferometrically, as a polarization phase difference instead of phase difference between two spatial different channels. UCI is close to the concept of Conoscopic Holography [10, 11], and like that method is expected to yield astonishing precision which is comparable to or

exceeding the precisions of a Michelson interferometer, while using a simpler and inherently stable set-up.

In this paper we introduce the UCI concept as a full two-dimensional astrometric imager. The same concept may be used to build a nulling interferometer or a simple fast one-dimensional astrometric imager.

### 1.3 *The calendar paradigm*

The UCI concept can be explained using a lunar calendar paradigm. The position of a star is measured as in a calendar, where the fine and crude information (months and years) are extracted separately using the moon and sun motions. Similarly, in UCI two complementary measurements are performed: a cruder one through the measurement of the position of the star in an intensity image and a fine interferometric polarization phase measurement.

The proposed system, orbiting in space on a satellite, observes at once a two-dimensional section of the sky through a telescope. The area covered by this observation is of the order of a fraction of a degree square. Each observation may last a few minutes to one hour. An adequate positioning system measures the absolute direction of the telescope central point for each exposure. The system is orbiting and scans the sky during a long period, typically five years, each segment of sky being observed and each star being detected and measured many times.

The system creates a set of data consisting, for each exposure, of two images. The first is an intensity image of the sky segment yielding in each shot, a large number of stars, at different positions in the segment, and with different magnitudes. The second is a phase image yielding the polarization phase created by the UCI at each pixel. Each star is first detected through the intensity image, from which a first position is calculated and this value is refined using the UCI data.

The intensity image is identical to the image obtained in a telescope, as Hypparcos or GAIA. It provides the position of each star, in both axes, through the detection of bright spots in the image. The system is designed such that the image of each star falls on a small number of pixels. The position of each star, in both axes, can be obtained with good resolution from the intensity image through calculation of the centroid of the energy distribution, as in similar systems[12]. The polarization phase image data is relevant only at positions of stars, as detected in the intensity image. Due to the reliance on the intensity image for star detection the polarization phase measurement will be meaningful only for stars resolved in the intensity image. In the intensity image, the resolution criterion is given mainly by the diffraction limit if an optical system well corrected for aberrations is used and it will also be the resolution limit of the system. At a star position, the polarization phase is proportional to the angle deviation of the star from the zeroth direction of the telescope. It provides the position of the star in one axis – the parallax direction - with high precision. The underlying assumption, as for other interferometric systems, is that the precise position in one axis contains a wealth of information. The angular dependent polarization phase is created in front of the telescope using a crystal assembly. The two steps measurement strategy relieves the tolerances and complexity of the second measuring step, after the creation of the polarization phase, to the level of standard imaging.

The acquired polarization is undisturbed by the subsequent optical elements if adequate care is taken in the optical design and assembly.

For each detected star, at each passage of the system, a record of the intensity derived position and of the polarization phase difference vs. the telescope absolute direction is kept for processing. The use of multiple exposures increases the precision of the system. In GAIA, which uses a similar paradigm, the accepted assumption is that an overall precision of  $10\mu\text{as}$  for the full mission can be reached with an instantaneous precision of  $100\mu\text{as}$  [6].

#### 1.4 Schematics of the system

A schematic of the system is presented in Figs. 1 and 2. The system is made of separate modules: A first module amplifies the incoming angle using achromatic anamorphic prisms. The polarization coding module differentiates the direction of the light by creating a polarization phase shift which depends on direction. The coding is done using birefringent crystals, as described below.

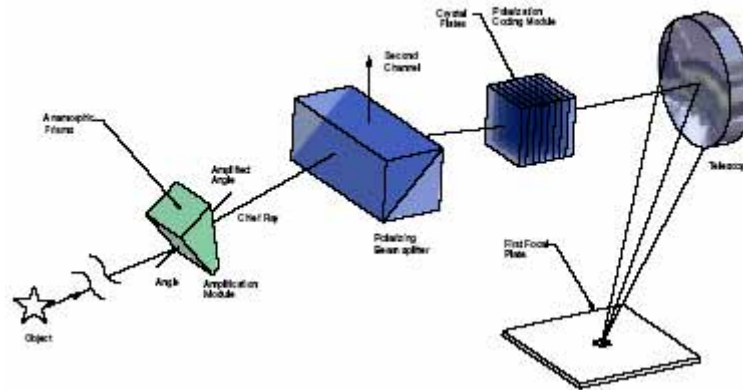


Fig. 1. Schematic of the system

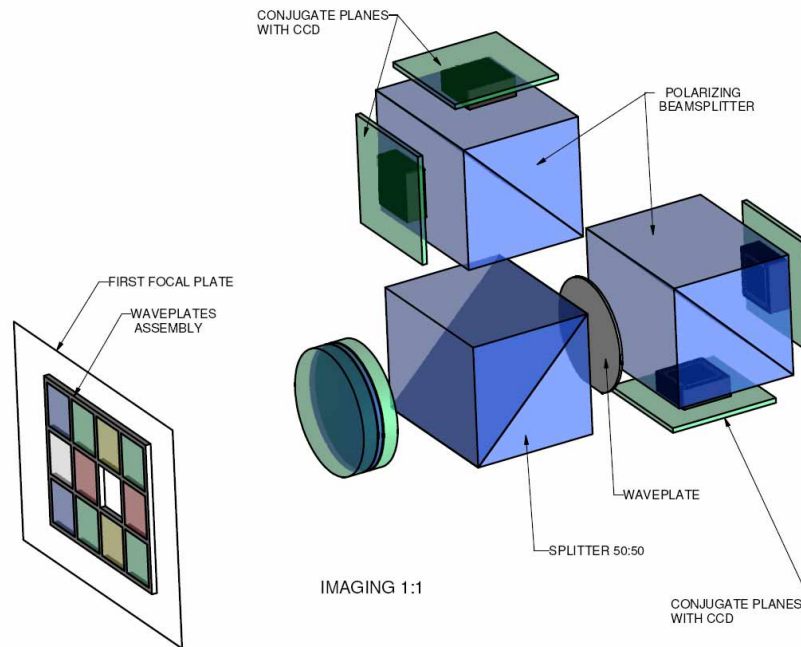


Fig. 2. Focal planes of the UCI

The telescope images the star on the first focal plane. At this plane the achromatization module is positioned. The polarimetric module creates a set of four images, each one representing a polarization state, of the focal plane, through a set of beamsplitters and waveplates (Fig. 2).

## 2. System description

First, an anamorphic prism is positioned at the entrance pupil. It increases the angular spread of the incoming light while reducing the optical aperture of the subsequent system.

A polarizing beamsplitter is used to separate the two incoming polarizations into two identical channels which may be used independently. Here we discuss only one of the channels.

Next, the heart of the device is an assembly of birefringent crystals. This assembly produces a polarization shift, which is a very sensitive measure of the angular position of the incoming light. A small shift in the angular position results in a polarization change which would be more than five orders of magnitude larger.

Next, the light passes through a telescope, which directs different angular regions into a set of detectors.

The achromatic corrector – described later – is positioned close to the first focal plane of the system. An additional lens assembly reimages the first focal plane on a second focal plane.

A non-polarizing beamsplitter separates the light evenly into two channels.

In one channel an additional quarter waveplate is introduced. A polarizing beamsplitter is positioned in each channel as an analyzer, creating overall four separate measuring channels. Four CCD image planes are used, one CCD for each channel. An intensity image is created numerically by adding the four images. In the intensity image, a star will ideally be represented by a small number of pixels determined by the Airy disk of the optical system. The precise polarization of the light impinging on the detector is then extracted and calculated. This is done by creating numerically a phase image using a four channels phase stepping algorithm. The combined information for the intensity and phase images gives the angular position of the star.

This optical set-up differs in several aspects from a Michelson stellar interferometer:

First, the UCI detects directly an angular change. The polarization phase difference depends directly on the angle, through the crystal optics relations. The angle is not an indirect variable retrieved through differentiation of two phases, separated geometrically.

Further, UCI is inherently stable even in the interferometric coding part, which for UCI is the crystal assembly. The two rays propagate along the same optical path and any relative disturbance is compensated efficiently. In any interferometer the constraint to keep two geometrically separated optical paths at the same relative position with subwavelength accuracy creates strong constraints on the mechanical design of the system. Because of this problem, standard interferometers have been limited to ultrastable environments and the use of interferometers outside the laboratory is limited. Conoscopic systems, which are closely related to UCI, are used in many applications, even in heavy industries including steel and automotive factories [13] and for industrial inline quality control, places where a Michelson interferometer will not be applicable.

The absolute crystal angular position has to be kept stable and monitored accurately because it is the reference of the system. Alternately, another star can be used as a reference, as used in many astrometric set-ups.

UCI is very sensitive. Static birefringence in uniaxial crystals is the only strong optical effect available along extended optical paths. This effect is associated with changes of relative index of refraction above 10% (e.g., in calcite), along paths of many centimeters. The only other optical effect reaching a change of index of refraction of 10% is based on liquid crystals but it can only be applied along paths way below one millimeter.)

The quality of the crystal is critical in this project. Any departure from an ideal crystal will be translated to a measurement error. This may be due to inhomogeneities of the birefringence, temperature variations or axis wobble as function of position. So far, work on conoscopic systems was limited to small crystals. The extension to large and thicker crystals, with high homogeneity, is a major challenge. Indeed, the development of large birefringent crystals with dimension above 100 mm is a huge engineering task.. Fortunately, this

development has already been performed by the NIF – National Ignition Facility – for KDP and DKDP crystals. These crystals have been recognized by the NIF as one of the key elements of laser fusion[14-16]

The performances and quality of crystals dedicated to laser fusion are similar to those required in UCI with the additional constraint of tolerating the high power passing through the crystals in laser fusion experiments. Through the NIF efforts, KDP crystals have been grown to sizes of 500 mm and birefringence homogeneities in the range of a few  $10^{-6}$ , on smaller crystals, have been obtained and reliably measured [17]. Stringent requirements are placed on characterizing, cutting and polishing the crystals [18]. The NIF goal is to industrially produce large crystals cheaply and at large quantities.

### 3. UCI functional description

#### 3.1 Polarization coding

A simplified ray optics description of light propagation in a uniaxial crystal will be used here.

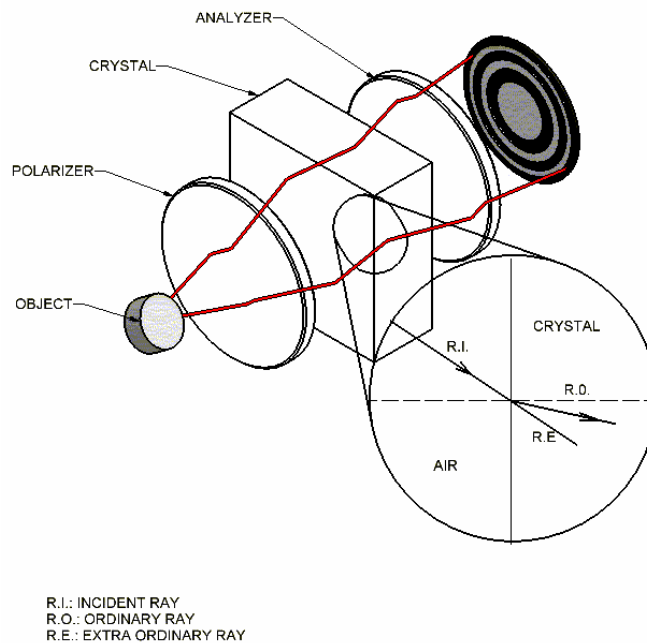


Fig. 3. Polarization coding – the drawing presents the case of an on-axis ( $\theta = 0$ ) crystal axis

A wave polarized at 45 degrees to the principal axes of the crystal is incident on it (Fig. 3). The wave is separated into two polarization components. In a uniaxial crystal the two polarized waves propagate at different velocities. The ordinary wave propagates at a velocity independent of the angle of the ray, while the extraordinary wave propagates at an angle-dependent velocity. A phase difference builds between the two waves along the path. This phase difference is a polarization difference and can be detected using polarimetric methods as described in the next section.

#### 3.2 Simplified polarization coding

Let a single ray impinge on the system. The incidence angles are labeled as  $\theta_x$  and  $\theta_y$  (Fig. 5) outside the crystal in the x and y directions respectively. Denote by  $\theta$  the angle of the crystal axis inside the crystal, in the xz plane. We can ignore the effects of the non-collinearity of the Poynting and extraordinary wave directions. We assume that the incidence angles are small relative to  $\theta$  and neglect also the difference in ray direction between the ordinary and

extraordinary waves. In this case, the angle of the ray relative to the crystal axis,  $\theta'$ , is approximately:

$$\theta' \simeq \theta + \frac{\theta_x}{n_{\text{eff}}}, \quad (1)$$

Where  $n_{\text{eff}}$  is an effective index of refraction chosen to be the geometrical mean of the ordinary and extraordinary indices of refraction at  $\theta$ :

$$n_{\text{eff}} = \sqrt{n_o n_e(\theta)} \quad (2)$$

The system is anamorphic – i.e., depends only on one axis, labeled here as x.

The dependence of the extraordinary index of refraction on the angle between the ray direction inside the crystal and the crystal axis is directly retrieved from the Fresnel equation of a uniaxial crystal[19]:

$$\frac{1}{n_e^2(\theta)} = \frac{\sin^2(\theta)}{n_e^2} + \frac{\cos^2(\theta)}{n_o^2}. \quad (3)$$

Defining the birefringence as  $\Delta n (= n_e - n_o)$ , it follows that:

$$\left. \frac{\partial(n_e(\theta))}{\partial\theta} \right| = - \frac{n_e^2(\theta) \sin(2\theta)}{2} \left[ \frac{1}{n_o^2} - \frac{1}{n_e^2} \right]. \quad (4)$$

Since  $\Delta n$  is small:

$$\left. \frac{\partial(n_e(\theta))}{\partial\theta} \right| = - \frac{\Delta n}{n_o} \sin(2\theta). \quad (5)$$

The phase difference is given then by:

$$\Delta\phi(\theta) = \frac{2\pi n_o L}{\lambda} - \frac{2\pi n_e(\theta) L}{\lambda}, \quad (6)$$

$L$  is the length of the crystal and  $\lambda$  is the wavelength. Rewriting leads to:

$$\Delta\phi(\theta) = \Delta\phi_0 + \frac{2\pi \Delta n L}{n_o \lambda} \sin(2\theta) \theta_x, \quad (7)$$

where the phase difference contains static and angle dependent terms.

### 3.3 Modified polarization coding

By using two crystals, each with the same angle-dependent term but with an opposite static term, the equation for a suitable combination of crystals is given by:

$$\Delta\phi(\theta) = \frac{2\pi \Delta n L_{\text{TOTAL}}}{n_o \lambda} \sin(2\theta) \theta_x, \quad (8)$$

where  $L_{\text{TOTAL}}$  is the aggregate length of the crystals. The module can use a single pair or several pairs, coupled with waveplates, to compensate for double refraction and to reduce the cost and the manufacturing tolerances.

The uniaxial angle ratio – UAR – is the ratio of the phase angle to the geometrical angle  $\theta_x$ :

$$UAR = \frac{2\pi \Delta n L_{TOTAL}}{n_o \lambda} \sin(2\theta) \quad (9)$$

The cycle angle,  $p_{cycle}$ , is the geometrical angle at the entrance of the system before the anamorphic prisms which is necessary to create a full cycle ( $2\pi$ ) of polarization angle; it is given by:

$$p_{cycle} = \frac{2\pi}{UAR * m} \quad (10)$$

Where  $m$  is the anamorphic prisms magnification.

### 3.4 Availability of crystals

The UCI performance will depend on the availability of large, highly birefringent crystals. Commercial standard crystals with high birefringence, such as natural calcite,  $\alpha$ -BBO or  $YVO_4$ , may reach 4-8 cm; however, larger crystals exist as synthetic calcite, lithium niobate crystals and lithium iodate. As explained above we choose to develop this project around KDP or DKDP crystals.

As a ballpark estimation, the overall optical aperture of the system, using DKDP crystals of 15\*15 cm and anamorphic prisms with a magnifying ratio of 5 The effective index of refraction of DKDP is 1.504 and the birefringence is 0.039. For  $\theta = 45^\circ$  and for an assembly of 20 pairs crystals of with each crystal from each pair having a length of 30 mm, i.e. total crystal length 1000 mm, the UAR is above  $3.2*10^5$ . • The overall volume of the crystal assembly will be 22 dm<sup>3</sup> and the weight will be 53 kg as the density of DKDP is 2.36 gm/cm<sup>3</sup> The absorption coefficient of KDP or DKDP is below 0.025 cm<sup>-1</sup> [20] (Fig. 3 here) between 425 and 750 nm so that the transmittance of a 1m long crystal stack is above 75%.

### 3.5 Polarimetric detection

Polarimetry in astronomy can be done in two fundamentally different ways [21, 22]. In one approach, DC polarimeters, the polarization is measured through an appropriate beamsplitter arrangement. A second approach, modulation polarimeters, is a temporal modulation where one chops between various states (of polarization, for instance). Temporal modulation has the advantage that the different states are observed with the same detector elements (pixels), which makes the normalized differences of states independent of the spatially varying detector gain.

Modern polarimeters use a combination of temporal and spatial modulation schemes. Systematic errors typically limit such instruments to a relative sensitivity of  $10^{-4}$ .

In the UCI project we plan to use a DC polarimeter with CCD. The CCD will use the TDI –Time Delay Integration – mode. In this mode the CCD charge is moved synchronously with the image movement creating a virtual pixel. This mode reduces pixel non-uniformities, as in the GAIA design. [12].

Let the four measurements be represented as:

$$I_j = A+B \cos(\theta + j \frac{\pi}{2}) + \delta I_j \quad (11)$$

where  $A$  and  $B$  are constants (taken here as equal),  $j$ , (ranging from 1 to 4), represents the four different detectors and  $\delta I_j$  represents the intensities errors, due to photon noise, in each detector. The total number of photons including all four detectors is the sum of the four intensities and is given by  $N = 4A$ , neglecting noise. The algorithm used is a four steps phase algorithm with steps equal to  $\pi/2$ . It can be shown [23] that the standard deviation of the phase error,  $\delta\theta$ , is given by

$$\overline{\langle (\delta\theta)^2 \rangle} = \frac{A}{2 B^2} = \frac{1}{2 A} = \frac{2}{N} \quad (12)$$

Where we used Eq.(5.7) in Ref. [23] and the values of  $w_j$  in Table 4 there for a four steps algorithm and for a CCD detector ( $k=1$ ).

### 3.6 Geometrical optics and interferometers

Usually the addition of geometrical imaging elements into interferometers is problematic. Indeed, any change in the wavefront through one of the telescopes compared to the other one in a Fizeau interferometer or any variation in the arms length in a Michelson stellar interferometer will add a sizeable error. The overall tolerance had been set to 25 pm for GAIA [9]. In UCI, however, the polarization phase information is superimposed on the light before any optically curved element is introduced. The remaining tolerances are that of a standard imaging telescope.

### 3.7 Diffraction effects in UCI

Diffraction effects in UCI can be calculated directly from the expansion of the incoming wave at the entrance stop. The overall diffraction effect will translate to an angular spread of some of the optical energy around the nominal direction. For a unapodized aperture stop the angular spread, around angle  $\theta_0$  for small angles, is given by the diffraction of a rectangular aperture:

$$I(\theta - \theta_0) = I_0 \frac{\sin^2\left(\frac{\pi D(\theta - \theta_0)}{\lambda}\right)}{\left(\frac{\pi D(\theta - \theta_0)}{\lambda}\right)^2} \quad (13)$$

However, one of the striking properties of phase measurement is that the measurement yields directly the center of gravity of any distribution, under the constraint that the spreading effect is small compared to the value of one cycle. Additionally, if the distribution is symmetrical, the center of gravity is identical to the original phase value. Under these conditions, the effect of the spread is therefore a small reduction of signal amplitude given by:

$$\eta = \frac{\int I(\theta - \theta_0) \cos\left(2\pi \frac{(\theta - \theta_0)}{cy}\right) d\theta}{\int I(\theta - \theta_0) d\theta} \quad (14)$$

so it is tolerable for small diffraction effects. For the system values presented below  $\eta$  is 84%.

### 3.8 Anamorphic prisms

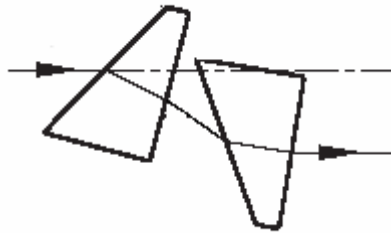


Fig. 4. Anamorphic prisms

Anamorphic prisms are used extensively in industry but are less common in research labs, except for laser diode circularization and in dye lasers. The description of the principle and parameters of achromatic anamorphic prisms can be found in [24, 25]

The main advantage of anamorphic prisms is the ability to increase – or reduce – the angular spread, using a relatively small optical length, without needing to pass through an optical curved element or a focal plane. Moreover, such prisms reduce the physical aperture of the system.

Anamorphic prisms are usually restricted to nearly collimated light since otherwise the magnification is dependent on the angle of incidence. In the system proposed here the light from a star is well collimated. Also, because the prisms are positioned at the entrance aperture any change of magnification will be translated to an image deformation, which can be corrected numerically.

The main issue in using anamorphic prisms in this design is their inherent chromaticity. To create an achromatic design, pairing of materials and angles has to be performed in order to remove the secondary and third color variations. A full design has to be performed in order to reach arc-second level of dispersion on typical values.

The final design may reach a magnification of 5-10 depending on the achromaticity target values and the number of prisms used and the details are beyond this paper's scope.

### 3.9 Anamorphism

The UCI system is anamorphic; it measures the angle in one dimension, as do Michelson stellar and Fizeau interferometers. The reason of this anamorphism in UCI is different than in a Michelson stellar interferometer. In the polarization coding, the measured angle is the angle  $\theta'$  between the ray and the crystal axis of the crystal. This angle is independent of the angle orthogonal to the plane comprising the crystal axis of the crystal and the geometrical axis of the system (Fig. 5).

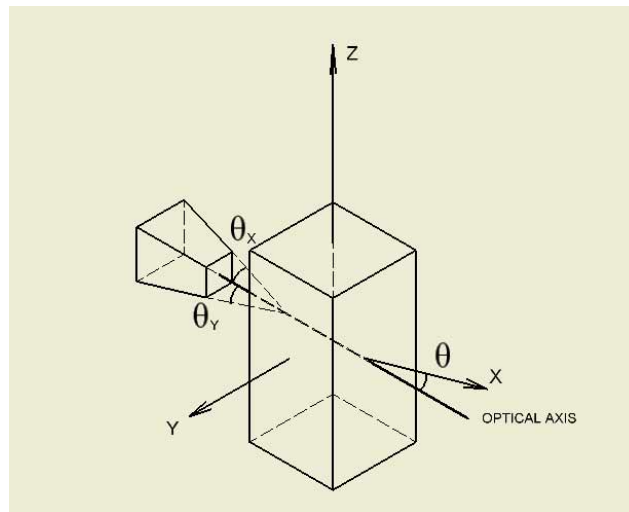


Fig. 5. Description of the system geometrical axis and crystal axis

### 3.10 Achromaticity and chromatic dependence

In astrometry each photon is important and the system needs to detect photons over a large wavelength range, typically from 0.4  $\mu\text{m}$  to 0.9  $\mu\text{m}$ . The star itself emits light in a narrower bandwidth, typically 100 nm, around its central wavelength. The central wavelength, the bandwidth and the star intensity are taken to be constant in time for most stars.

The polarization coding module is fully achromatic in one dimension at  $\theta' = 0$ , and departs linearly from achromaticity with increasing angle in the x direction. The polarization phases of the same star and the system absolute position are measured many times throughout the mission. For each star, the results will be formatted as a graph of  $\Delta\phi$ , the measured polarization phase as function of  $\theta$ , the absolute position of the system. Following (8), the graph will be linear with the intercept of the graph representing the star position. The slope of the graph, equal to the UAR (9), depends on the central wavelength and permits to retrieve this parameter. Alternatively, if the slope is known, fewer points are needed for retrieving the star position.

When the polarization phase,  $\Delta\phi$ , departs too much from the zero phase point the spread around the central wavelength will reduce the signal because the different wavelengths will produce markedly different polarization phases. To avoid this limitation, which will reduce the angular field of the system in one dimension, two solutions will be used in combination:

First, the phase will be reset to zero periodically as function of the angle. This can be done by using a “chessboard” of waveplates positioned at the first focal plane (Figs. 2 and 6). The thickness of each waveplate cancels exactly the phase created at the geometrical center of the waveplate. By using the same crystal as for the polarization coding module we cancel exactly at this point the phase for any wavelength. In this case the thickness of waveplate (i,j) is simply given by  $UAR * \theta_{ij}$ , where  $\theta_{ij}$  being the angular position in the sky represented by the geometrical center of the waveplate (i,j).

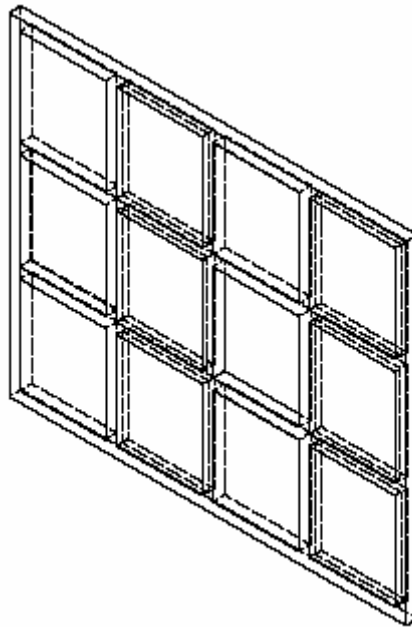


Fig. 6. Achromatization system layout. The illustration presents a 4x3 waveplates assembly. In a real system a much larger number of waveplates will be used.

The size and number of waveplates depends on the additional achromatization provided by the system. Several solutions exist and need to be evaluated in more details.

First it is possible to disperse the star energy in the orthogonal dimension to create a small spectrum and to reduce the wavelength spread around each point. This solution has been proposed in DIVA and in the earliest versions of GAIA [26, 27] to solve a similar problem.

Additionally, the birefringence dispersion can be used in a scheme similar to the design of achromatic waveplates [28]. By choosing two crystals with very different dispersions it is possible to create a **chromatic** waveplate with **zero** phase difference at the central wavelength. By modifying the thickness of this waveplate it is possible to obtain a fixed chromatic birefringence which cancels the dispersion of Eq. (8).

Polarizing beamsplitters which are achromatic on the full visible range are available commercially. The main source for chromaticity, therefore, is the anamorphic prisms. The standard anamorphic prisms, used in laser diode circularization, are strongly dispersive. Achromatic anamorphic prisms have been developed for dye lasers and femtosecond optics. By a proper choice of angles and materials, a two-prism design can cancel the first order dispersion and minimize the second order. More evolved designs using several prisms can be performed but with an additional complexity of the prism. A full design of the achromatic anamorphic prism is beyond the scope of this paper in which we take the anamorphic ratio to be 5.

#### 4. Expected performance

We present here a ballpark estimation of the performances.

##### 4.1 Quantity of light

A full account of the quantity of light will be performed later; for a rough estimate the main parameter is the aperture, limited by the crystal sizes.

As an estimate, the overall aperture, if anamorphic prisms with a magnification ratio of 5 are used, may reach 75cm by 15 cm for KDP crystals...

The system differs from imaging systems and interferometers in that half of the energy is used due to the entrance polarizer, although the second half may be used as a separate channel.

##### 4.2 Angular resolution

As stated before for an overall mission precision of 10  $\mu$ as an instantaneous precision of 100  $\mu$ as is requested [6].

An anamorphic prisms module, with magnification of 5, will translate an instantaneous 100  $\mu$ as change of the position of a star to 500  $\mu$ as or 2.5 nrad.

For the KDP crystal assembly described before the uniaxial amplification ratio of  $3.2 \cdot 10^5$ , i.e., a 2.5 nrad change of geometrical angle translates to a change of 0.8 mrad of polarization angle.

The detectivity of the proposed system is limited by the number of photons available. Eq. (12) gave the phase error as function of the number of overall photons reaching one of the four detectors. To reach 0.8 mrad error the number of photons reaching the detectors has to be  $3 \cdot 10^6$ . Taking into account system losses the number of photons at the entrance of the system has to be larger than  $10^7$ . The limit of detectivity for the overall mission can then reach close to 10  $\mu$ as for a high photon flux ( $5 \cdot 10^7$  photons per exposure), 100  $\mu$ as for medium photon flux ( $5 \cdot 10^5$  photons per exposure) and 1mas for low photon flux ( $5 \cdot 10^3$  photons per exposure).

##### 4.3 Angular channel

For a 75\*15 cm aperture The optical diffraction limit is in the x and y directions 0.15 and 1 arcsecond. This should be compared with the angle for a full cycle,  $p_{\text{cycle}}$ , which was estimated above to be 4 $\mu$ rad or 0.8 arcsecond. As explained above the optical diffraction creates a symmetric angular spread around the nominal angular value. This spread reduces slightly the signal strength (Eq. (14)).

In the x direction a first magnification of 5 is applied through the anamorphic prisms.

Assuming the focal length of the telescope to be 5 m (a relatively easily obtainable value) in the y direction, 1 arc second will translate to 25  $\mu$ m. In the x direction the effective focal

length – including the anamorphic prisms magnification – is 25 m. In the x direction the same 1 arc second will translate to 125  $\mu\text{m}$ .

## **5. Conclusions**

We presented the basics of a new method of imaging astrometry. While major technical challenges remain, the approach has several inherent advantages which makes it a candidate for astrometry. UCI is very simple to construct and uses the natural interference over an extended range within uniaxial crystals rather than the interference between two spatial paths in most traditional interferometers. A single path is used so the size and tolerances are relieved; polarization phase is measured rather than a phase difference, thereby reducing noise values. A future paper will describe the details of the system and report results of a preliminary study showing the potential angular resolution of UCI. In another future paper we will describe the use of the UCI concept as a coronagraph for detecting planets in vicinity of stars.

## **Acknowledgments**

We thank Nataly Beider for making several drawings and the NSF and PRF for support. Helpful comments by Ned Wright and by the referees are gratefully acknowledged.